STABILITY ANALYSIS OF COMPOUND TCP WITH ADAPTIVE VIRTUAL QUEUES

A Project Report

submitted by

ANAND KRISHNAMURTI RAO

(EE09B005)

in partial fulfilment of the requirements
for the award of the degree of

BACHELOR OF TECHNOLOGY
in
ELECTRICAL ENGINEERING

DEPARTMENT OF ELECTRICAL ENGINEERING
INDIAN INSTITUTE OF TECHNOLOGY, MADRAS.

May 14, 2013

PROJECT CERTIFICATE

This is to certify that the project titled **STABILITY ANALYSIS OF COMPOUND TCP WITH ADAPTIVE VIRTUAL QUEUES**, submitted by **Anand Krishnamurti Rao (EE09B005)**, to the Indian Institute of Technology, Madras, for the award of the degree of **Bachelor of Technology**, is a bona fide record of the project work done by him under my supervision. The contents of this report, in full or in parts, have not been submitted to any other Institute or University for the award of any degree or diploma.

Prof. G. Raina
Project Guide
Professor
Dept. of Electrical Engineering
IIT Madras, Chennai 600 036

Prof. E. Bhattacharya
Head
Dept. of Electrical Engineering
IIT Madras, Chennai 600 036

Place: Chennai

Date: May 14, 2013

ACKNOWLEDGEMENTS

I would first like to thank Dr. Gaurav Raina for his guidance throughout the course of this project. He has taught me the importance of framing a scientific argument along with presenting sound analysis.

Special thanks to Amit Warrier, my batchmate, with whom I have worked with for a year in completing this project.

I also thank my parents and friends who have been there as a constant source of support in all my endeavours.

This work was carried out under the IU-ATC project funded by the Department of Science and Technology (DST) Government of India and the UK EPSRC Digital Economy Programme.

ABSTRACT

KEYWORDS: Compound TCP; virtual queue management; non-linear systems; local stability; Hopf bifurcation.

Compound TCP (C-TCP) is currently the default transport layer protocol in the Windows operating system. We study a non-linear fluid model of Compound along with Virtual Queue (VQ) management schemes in network routers. One can implement virtual queue policies either non-adaptively or adaptively. The Adaptive Virtual Queue (AVQ), in particular, has the objective of driving the link utilisation to a desired level.

The stability analysis of non-adaptive virtual queues reveals that smaller virtual buffer sizing rules help stability. Small virtual buffers would quite naturally reduce queueing delays in routers. Some guidelines for Compound and network parameters to ensure local stability are outlined. Analysis of the AVQ policy shows that the system is prone to losing local stability with large feedback delays, high link capacities, and with variations in the AVQ damping factor. We further show that the loss of local stability would occur via a Hopf bifurcation. Based on the analysis, our recommendation is that a virtual queue, with small buffer sizes, could be an attractive queue management scheme.

TABLE OF CONTENTS

ACKNOWLEDGEMENTS **i**

ABSTRACT **ii**

LIST OF FIGURES **iv**

ABBREVIATIONS **v**

1 Introduction **1**

2 Models **3**

2.1 Compound TCP 3

2.2 Virtual Queues 4

2.3 Adaptive Virtual Queue 6

3 Analysis **8**

3.1 Virtual Queues 8

3.2 Adaptive Virtual Queue 12

4 Outlook **19**

A Analytical characterisation: stability and periodicity of bifurcating solutions **21**

LIST OF FIGURES

2.1 The *real queue* has the capacity to serve C packets per unit time and can hold B packets in its buffer. The service rate and the buffer size of the *virtual queue* are scaled down by a factor $\kappa < 1$. We assume there is a time delay of τ time units before any feedback is received by the end-systems. 5

3.1 Marking probability of the virtual queue model (3.4), with variations in B/σ^2. Note that smaller buffer thresholds provide early indications of congestion as the load increases. 10

3.2 Stability factor of the virtual queue (3.4), with variations in buffer thresholds and the Compound parameter α. Note that both the buffer size B and the parameter α influence stability. We used $C = 100, \sigma = 1, \beta = 0.5, k = 1$. 12

3.3 Local stability chart of the C-TCP/AVQ model. The area below the curves represents the stable region. Note the trade-offs among the system parameters to maintain stability. Variations in the AVQ damping factor θ can induce a Hopf bifurcation. Compound parameters: $\alpha = 0.125$, $\beta = 0.5$, $k = 0.75$. 17

A.1 Bifurcation diagram generated with variation in damping factor θ. The Hopf is found to be subcritical, and the limit cycles unstable (A.31). 32

ABBREVIATIONS

AQM	Active Queue Management
AVQ	Adaptive Virtual Queue
C-TCP	Compound Transmission Control Protocol
ECN	Explicit Congestion Notification
IP	Internet Protocol
QoS	Quality of Service
RED	Random Early Detection
REM	Random Exponential Marking
VQ	Virtual Queue

CHAPTER 1

Introduction

The design of transport protocols influences the performance of Internet applications. Active Queue Management (AQM) schemes, which aim to provide timely indications of incipient congestion in the network to end-systems, also play an important role in Quality of Service (QoS). For an end-to-end perspective, it is natural to study the interaction of a transport protocol along with a queue management scheme. Compound TCP (C-TCP) (17) is today widely implemented in the Windows operating system, and there are numerous proposals for AQMs in the literature.

Queueing delay, in the Internet, is undesirable and specially hurts the performance of delay sensitive applications (11). It is being recognised that network latency is predominantly due to large router buffers without effective queue management (4). It is difficult for end-systems to compensate for queueing delay, and thus the design of AQMs remains an important aspect of network research. A number of AQM schemes, with different objectives, have been proposed in the literature. For example, Random Early Detection (RED) (3) strives for *small average queue sizes*, Adaptive Virtual Queue (AVQ) (10) targets a *desired link utilisation*, Random Exponential Marking (REM) (1) aims for both *small queue sizes* and *high link utilisation*, and CODEL (11) specially aims to *control queueing delay*. However, a simple Drop-Tail queue policy is often used as there is no consensus on an optimal AQM scheme. Drop-Tail, as the name suggests, simply drops packets that arrive to find a full buffer. For our study, we focus on a class of virtual queue schemes as they aim to provide early indications of congestion. We study a non-adaptive Virtual Queue (VQ) (9) and the Adaptive Virtual Queue (AVQ) (10).

Stability is a key performance metric since feedback, from the network to end-systems, is usually time delayed. So the analysis of non-linear, time delayed, fluid models for transport protocols can help guide protocol or network

parameters, and ensure system stability. For example, non-linear models of TCP Reno have been studied with different buffer sizing regimes (14) (15), with the AVQ (10), and also with Drop-Tail (12). These papers have highlighted that the underlying models can readily lose stability with variations in system parameters. Hence any analysis should consider both *stability* and *bifurcation* phenomena (6).

In this paper, we analyse a recently proposed non-linear model of Compound (16) with a VQ (9) and with the AVQ (10). Local stability analysis with the VQ policy reveals that *smaller virtual buffer* sizing rules help stability. Small virtual buffers would also lead to lower latency in network routers. We outline some guidelines for Compound and network parameters to ensure local stability. Analysis of the AVQ shows that the system could readily lose local stability with large delays, high link capacities, and with variations in the AVQ damping factor. We show that loss of local stability would occur via a Hopf bifurcation (8), which would give rise to a limit cycle. Based on the analysis, we note that a virtual queue, with small buffer sizes, could be an appealing queue management policy.

The rest of this paper is organised as follows. In Section 2, we outline models for Compound and for virtual queue management schemes. In Section 3 we conduct a stability analysis of the underlying models, and summarise our contributions in Section 4.

CHAPTER 2

Models

In this section, we outline models for Compound and the virtual queue policies that form the basis for our analysis.

2.1 Compound TCP

The following *many flows*, non-linear, fluid model has been proposed for a generalised TCP (14):

$$\frac{dw(t)}{dt} = \Big(i\big(w(t)\big) - d\big(w(t)\big)p(t-\tau)\Big)\frac{w(t-\tau)}{\tau}, \tag{2.1}$$

where $w(t)$ is the congestion window, $i(w(t))$ is the increase in $w(t)$ per *positive* acknowledgement, $d(w(t))$ is the decrease in $w(t)$ per *negative* acknowledgement, $p(t)$ represents an appropriate model at the resource, and τ is the feedback delay of the TCP flows present. An approximation for the average rate at which packets are sent is $x(t) = w(t)/\tau$.

In the regime where the queueing delay forms a negligible component of the end-to-end delay, the following functional forms have been proposed for Compound (16):

$$i\big(w(t)\big) = \frac{\alpha w(t)^k}{w(t)}, \qquad d\big(w(t)\big) = \beta w(t), \tag{2.2}$$

where the parameters α, β and k influence the congestion window's scalability, smoothness and responsiveness respectively. The default values of these parameters are: $\alpha = 0.125$, $\beta = 0.5$ and $k = 0.75$ (16). It should be noted that the fluid model is valid when there are many simultaneous TCP flows present in a high bandwidth-delay product environment.

The simplest queue management policy is Drop-Tail. In a regime where the number of users are large, and the router buffer sizes are small, a simple fluid

model for Drop-Tail is (15):

$$p(t) = \big(x(t)/C\big)^B, \tag{2.3}$$

where B is the buffer size and C is the link capacity. For the requisite queueing theoretic arguments behind the derivation of this fluid model the reader is referred to (15). Later in the paper, we will outline the impact this queue policy can have on local stability.

2.2 Virtual Queues

Virtual queues have been proposed as possible queue management schemes; for an early discussion on virtual queues, see (5). Figure 2.1 shows a basic virtual queue algorithm. Packets arriving at the queue are added unless the buffer occupancy exceeds B packets. A *virtual* queue operates with a service rate and a buffer size that are both less than the *real* queue. The algorithm has a parameter, $0 < \kappa \leq 1$, which can be tuned by the network provider. Any arriving packet that would lead to the virtual queue exceeding the value κB is marked to indicate the onset of congestion. Packets can also be dropped when the virtual queue crosses the virtual buffer size. End-systems will realise that their packets have been marked, or dropped at the queue, only after some time delay. The central idea, for virtual queues, is to start giving early indications of incipient congestion whenever the rate of offered traffic nears κ.

As a simple model, let us assume that the arriving traffic is a Poisson process. The server will then just be an M/D/1/B queue. Consider an M/D/1/B queue with arrival rate λ and a service every n units of time. The number of packets in the queue, just after each service, forms a Markov process and it is a straightforward exercise to calculate the stationary distribution of the process. So we can readily deduce the packet *loss* probability and the *utilisation* of the server. Such calculations would allow the network provider to better understand the trade-offs between loss and utilisation. As feedback from the queue to the end-systems is time delayed, another performance metric to consider is stability.

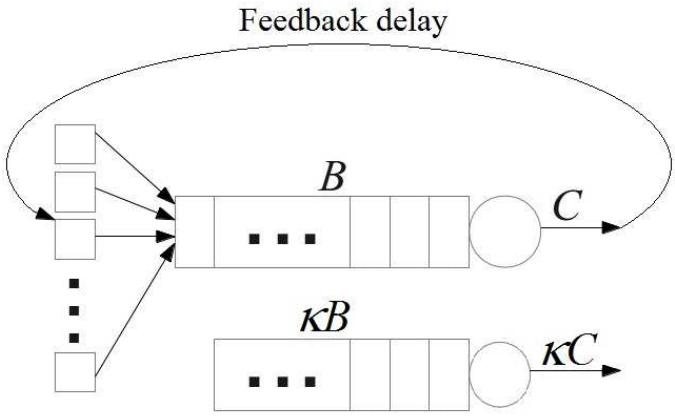

Figure 2.1: The *real queue* has the capacity to serve C packets per unit time and can hold B packets in its buffer. The service rate and the buffer size of the *virtual queue* are scaled down by a factor $\kappa < 1$. We assume there is a time delay of τ time units before any feedback is received by the end-systems.

We now outline a model proposed in (9). Assume that a virtual buffer of finite size B is maintained, and that from the time of a virtual buffer overflow to the end of the virtual buffer's busy period, all packets leaving the real queue are marked. Thus the virtual buffer's contents evolve as if overflow is lost, while the real buffer may or may not have loss. Consider a *Gaussian traffic model*: suppose that the workload arriving at the resource over a time period δ is Gaussian, with mean $x\delta$ and variance $x\delta\sigma^2$. For this model, the rate at which workload exceeds the virtual buffer is (7)

$$L(x, C) = (C - x)\left(\exp\left\{\frac{2B(C-x)}{x\sigma^2}\right\} - 1\right)^{-1},$$

and the proportion of workload marked is

$$p(t) = -\frac{d}{dC}L\big(x, C\big),$$

which reduces to

$$p\,(t) = \frac{r(t)e^{r(t)} - e^{r(t)} + 1}{\left(e^{r(t)} - 1\right)^2},$$

where $r(t) = \frac{2B\left(C - x(t)\right)}{\sigma^2 x(t)}$.

For the purpose of analysis and discussion, in this paper, we refer to the above virtual queue based scheme as a non-adaptive Virtual Queue (VQ). We now describe the Adaptive Virtual Queue (AVQ) policy which explicitly aims

for a desired and high link utilisation (10).

2.3 Adaptive Virtual Queue

Virtual queue management aims to provide early indications of congestion in the network. This idea was extended to strive for high link utilisation through the notion of an Adaptive Virtual Queue (AVQ) (10). The AVQ maintains a virtual buffer whose size is the same as the real buffer. However, there is a virtual capacity which is less than the real capacity, and this is *adapted* at the queues to achieve high link utilisation.

At the *packet-level*, the AVQ is implemented as follows (10): when a packet arrives, a fictitious packet is added to the virtual queue, if it is not already full. If there is an overflow, the packet is discarded from the virtual queue and marked/dropped in the real queue. At the *fluid-level*, the marking probability $p(t)$ is expressed in terms of the rate $x(t)$ as well as the virtual capacity $\tilde{C}(t)$. The following functional form for the marking probability at the resource was proposed in (10):

$$p(t) = \frac{\max\{0, \big(x(t) - \tilde{C}(t)\big)\}}{x(t)}, \tag{2.4}$$

where this function is differentiable in the region $x > \tilde{C}$. The virtual capacity $\tilde{C}$ is updated after every arrival epoch to achieve a desired utilisation. The AVQ update model, at the router, is

$$\frac{d\tilde{C}(t)}{dt} = \theta\bigg(\gamma C - x(t)\bigg),$$

where $\theta > 0$ is the *damping factor* and $\gamma \leq 1$ allows one to choose the desired *utilisation*. The factor θ determines how fast the marking probability adapts to changing network conditions, and its choice is important to maintain *stability*. Marking of packets is more aggressive when link utilisation exceeds the desired level, and less aggressive otherwise. In the functional form (2.4) for the marking probability, instead of adapting the virtual capacity we could use a static virtual capacity which is strictly less than the real capacity.

Some key features of the AVQ scheme, which are different to the well-studied RED proposal (3) are as follows: (i) The AVQ marks packets according to the *rate*, and not the queue length or average queue length; (ii) The scheme explicitly regulates the link utilisation, and not the queue length; (iii) The virtual capacity is modified by the AVQ update model, and random number generations at the queue to determine decisions to drop packets are not required.

The Compound fluid model (2.1) coupled with the AVQ update model for the virtual capacity forms an end-to-end, non-linear, dynamical system. The stability analysis of this system can help us understand trade-offs for design, and guide parameters to ensure stable operation. A local stability analysis of TCP Reno coupled with the AVQ model has been conducted in (10). Our focus is on Compound TCP, and in the next section we study some stability properties of both non-adaptive virtual queues and the AVQ scheme.

CHAPTER 3

Analysis

In Section 3.1, we study some non-adaptive queue policies and in Section 3.2, we analyse the AVQ policy with Compound TCP.

3.1 Virtual Queues

We recapitulate the fluid model for generalised TCP (2.1):

$$\frac{dw(t)}{dt} = \Big(i\big(w(t)\big) - d\big(w(t)\big)p(t-\tau)\Big)\frac{w(t-\tau)}{\tau}.$$

The function $p(t)$ represents packet loss or marking probability of packets sent at time t. The TCP increment and decrement functions are $i(w)$ and $d(w)$ respectively. Recall that the approximation for the average rate of sending packets is $x(t) = w(t)/\tau$, where τ is the feedback delay of TCP flows. The above model achieves equilibrium at

$$i(w^*) = d(w^*)p^*,$$

where w^* and p^* denote the steady state window size and the packet loss respectively. For linearising the generalised TCP equation, consider $w(t) = w^* + u(t)$, where $u(t)$ is a small perturbation. This gives

$$\frac{du(t)}{dt} = -au(t) - bu(t-\tau), \tag{3.1}$$

where

$$a = -\frac{w^*}{\tau}\left(i' - d'p^*\right)$$
$$b = \frac{1}{\tau}\left(d(w^*)w^*p'\right).$$

Note that $p' = \frac{dp}{dw}\big|_{w=w^*}$; i' and d' are similar representations. For Compound TCP, the functional forms for $i(w)$ and $d(w)$ are outlined in (2.2). Substituting

these expressions into (3.1) gives

$$\begin{aligned} a =& -(k-2)\frac{\alpha w^{*k-1}}{\tau} \\ b =& \frac{\alpha w^{*k-1}}{\tau}\frac{w^* p'}{p^*}, \end{aligned} \tag{3.2}$$

where α, β and k are Compound parameters. Under the constraints that $b > a \geq 0$ and $\tau > 0$, a *sufficient condition* for local stability of the linear system (3.1) is (13)

$$b\tau < \pi/2. \tag{3.3}$$

We will refer to $b\tau$ as the *stability factor*. In our build up towards studying a non-adaptive virtual queue (3.4) with Compound TCP, we first analyse two simple models for the queue.

In a *many flows* regime, when the bandwidth-delay product is large and the router buffers are small, the following fluid-level approximation has been proposed for Drop-Tail queues (15):

$$p(t) = \big(x(t)/C\big)^B.$$

Here B is the router buffer size and C is the link capacity. In this model there is no explicit adaptation at the resource, and with Compound there is no control over link utilisation. In this regime, it is assumed that the queue size fluctuates so rapidly that TCP cannot control the queue size. In fact, it can only control its distribution, and hence an explicit representation for the instantaneous queue size does not feature in the model.

With the small buffer Drop-Tail model, a *sufficient* condition for local stability with Compound is (16)

$$\alpha {w^*}^{k-1} B < \pi/2.$$

Note that this condition does not depend on the feedback delay or the link capacity, but depends on the buffer size and the Compound parameters. This very simple model alerts us to the fact that with large buffers the system could be harder to stabilise.

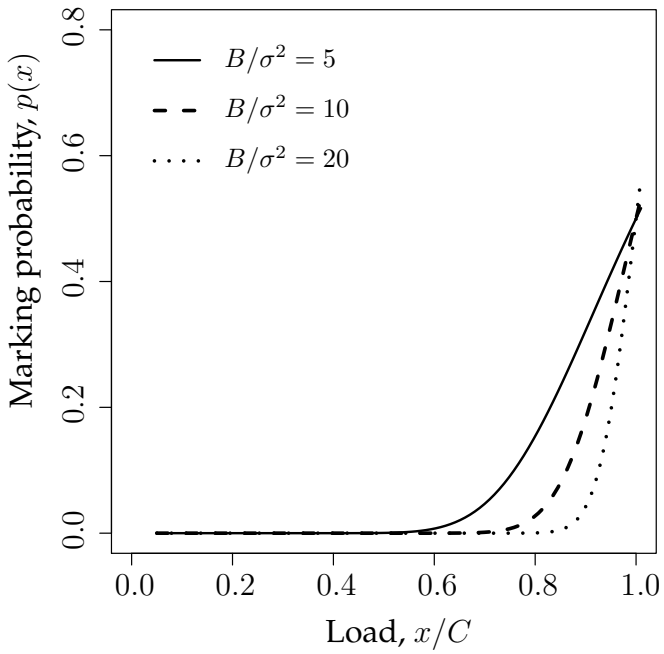

Figure 3.1: Marking probability of the virtual queue model (3.4), with variations in B/σ^2. Note that smaller buffer thresholds provide early indications of congestion as the load increases.

We now consider a functional form for the resource, outlined in Section 2, and proposed by (10):

$$p(t) = \frac{\max\{0, \big(x(t) - \gamma C\big)\}}{x(t)},$$

where $\gamma < 1$, C is the link capacity, and there is no adaptation at the links. For this resource model, $p(\cdot)$ represents the proportion of packets overflowing a *large buffer*. With this functional form, the corresponding sufficient condition for local stability with Compound is (16)

$$\beta\gamma C\tau < \pi/2.$$

This condition would clearly be difficult to satisfy with large feedback delays and high link capacities. The models considered so far suggest that both Compound and network parameters can readily influence stability. In particular, buffer sizes play an important role and need to be chosen judiciously.

The marking probability for the virtual queue policy outlined in Section 2,

under a Gaussian traffic model, is

$$p(t) = \frac{r(t)e^{r(t)} - e^{r(t)} + 1}{\left(e^{r(t)} - 1\right)^2}, \tag{3.4}$$

where $r(t) = \frac{2B\left(C - x(t)\right)}{\sigma^2 x(t)}$.

Figure 3.1 depicts the marking probability, of this model, for varying values of the buffer size. Note that smaller values of B provide early indications of congestion, as the load on the system increases. With $k = 1$, the sufficient condition for stability is simply $\alpha w p'/p < \pi/2$, at equilibrium. Observe the important role played by the derivative of the function p in maintaining stability. Substituting (3.4) into the fluid model for Compound, a sufficient condition for local stability can be written as

$$\left(\frac{(r^* - 2)\, e^{2r^*} + (r^* + 2)\, e^{r^*}}{(e^{r^*} - 1)\,(r^* e^{r^*} - e^{r^*} + 1)}\right) \frac{C}{x^*} \frac{2\alpha B}{\sigma^2} < \pi/2,$$

where $r^* = \frac{2B(C - x^*)}{\sigma^2 x^*}$. For stability there appears to be a requirement to jointly design the protocol parameter α and the network parameter B. Larger values of σ^2, the variability of the traffic at the packet-level, appears to help stability. In Figure 3.2, we plot the stability factor for different values of the Compound parameter α and the buffer size B. Note that both B and α have to be judiciously chosen to ensure stability.

When the buffer threshold levels used to mark/drop packets are large enough so that queueing delays are comparable to propagation delays, the above models do not accurately represent the resource. In such a regime, it is important to model both the instantaneous queue size and the end-system rates in any dynamic representation. The reader is referred to (14) (15) for the development, and analysis, of some such models. With the models considered so far, we find that small buffer sizes help maintain stability, and reduce latency, but there is no explicit control over link utilisation. High link utilisation is one of the key aims of the AVQ, and this model will now be analysed.

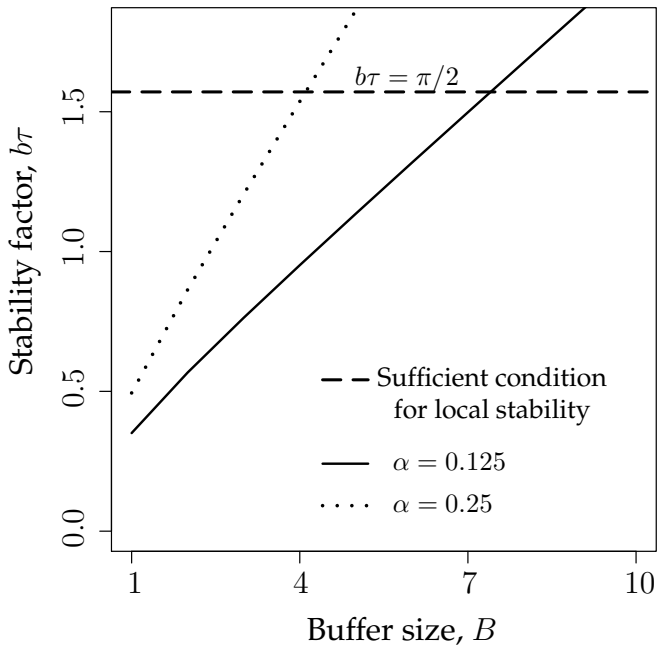

Figure 3.2: Stability factor of the virtual queue (3.4), with variations in buffer thresholds and the Compound parameter α. Note that both the buffer size B and the parameter α influence stability. We used $C = 100, \sigma = 1, \beta = 0.5, k = 1$.

3.2 Adaptive Virtual Queue

We now study Compound TCP with the AVQ policy whose objective is to target a high link utilisation. The C-TCP/AVQ system is represented by the following equations

$$\begin{aligned} \frac{dw(t)}{dt} &= \Big(\alpha w(t)^{k-1} - \beta w(t) p(t-\tau)\Big) \frac{w\,(t-\tau)}{\tau} \\ \frac{d\tilde{C}(t)}{dt} &= \theta\Big(\gamma C - x(t)\Big), \end{aligned} \tag{3.5}$$

where the marking probability takes the form (10)

$$p(t) = \frac{\max\{0, (x(t) - \tilde{C}(t))\}}{x(t)}.$$

Recall that $x(t) = w(t)/\tau$, where $w(t)$ is the congestion window, $x(t)$ denotes the total flow into the link, and τ represents the feedback delay. The virtual capacity of the link is represented by $\tilde{C} \leq C$. The default values of the Compound parameters are $\alpha = 0.125$, $\beta = 0.5$ and $k = 0.75$. The AVQ parameter $\gamma \leq 1$ determines the link utilisation, and $\theta > 0$ influences stability.

To study *local* stability, we first linearise system (3.5) about equilibrium. We

then derive the associated characteristic equation, and identify conditions under which the roots lie in the left-half plane (i.e., if Γ is a root, $\text{Re}(\Gamma) < 0$).

At steady state, $\frac{dw(t)}{dt} = \frac{d\tilde{C}(t)}{dt} = 0$. Therefore

$$w^* = \tau\gamma C, \quad \tilde{C}^* = \gamma C\left(1 - \frac{\alpha}{\beta}(\tau\gamma C)^{k-2}\right) \tag{3.6}$$

which uniquely defines the equilibrium window size w^* and virtual capacity $\tilde{C}^*$ in terms of parameter values. To linearise the coupled system (3.5), let

$$\begin{aligned} w(t) &= w^* + u(t) \\ \tilde{C}(t) &= \tilde{C}^* + v(t), \end{aligned}$$

where u and v are small increments of w^* and $\tilde{C}^*$. We get

$$\begin{aligned} \frac{du(t)}{dt} &= \left(\frac{\alpha}{\tau}(k-2)w^{*k-1}\right)u(t) + \left(\frac{\beta}{\tau}w^*\right)v(t-\tau) \\ &\qquad + \left(\frac{\alpha}{\tau}w^{*k-1} - \frac{\beta}{\tau}w^*\right)u(t-\tau) \\ \frac{dv(t)}{dt} &= -\frac{\theta}{\tau}u(t). \end{aligned}$$

To obtain the characteristic equation of this linearised system we look for exponential solutions, $v = Ae^{\lambda t}$, to get

$$\lambda^2 + a_0\lambda + a_1\lambda e^{-\lambda\tau} + \theta a_2 e^{-\lambda\tau} = 0, \tag{3.7}$$

where

$$\begin{aligned} a_0 &= -\frac{\alpha}{\tau}(k-2)(\tau\gamma C)^{(k-1)} \\ a_1 &= -\frac{1}{\tau}\left(\alpha(\tau\gamma C)^{(k-1)} - \beta\tau\gamma C\right) \\ a_2 &= \beta\gamma C, \end{aligned}$$

are assumed to be positive, and $\lambda = \sigma + j\omega$.

Local stability analysis

Consider the characteristic equation

$$\lambda^2 + a_0\lambda + a_1\lambda e^{-\lambda\tau} + \theta a_2 e^{-\lambda\tau} = 0, \tag{3.8}$$

where $a_0, a_1, a_2 > 0$ are independent of the feedback delay τ and $\theta > 0$. It is straightforward to show that when $\tau = 0$, all roots have negative real part and so the corresponding linear system is stable. The roots of (3.8) are continuous functions of system parameters. By keeping all the other parameters constant and increasing τ, one can locate a $\widehat{\tau}$ such that at least one of the roots hits the imaginary axis. Thus for $0 \leq \tau < \widehat{\tau}$, the roots of (3.8) will all have negative real parts.

When one of the roots first lies on the imaginary axis, $\sigma = 0$. At this point, let $\omega = \omega_0$. The real and imaginary parts of (3.8) are, respectively,

$$\omega_0 a_1 \sin(\omega_0\tau) + \theta a_2 \cos(\omega_0\tau) - \omega_0^2 = 0 \tag{3.9}$$

$$\omega_0 a_1 \cos(\omega_0\tau) - \theta a_2 \sin(\omega_0\tau) + a_0\omega_0 = 0. \tag{3.10}$$

Squaring and adding (3.9) and (3.10) yields

$$\omega_0^2 = \frac{(a_1^2 - a_0^2) + \sqrt{(a_1^2 - a_0^2)^2 + 4(\theta a_2)^2}}{2}. \tag{3.11}$$

Eliminating $\sin(\omega_0\tau)$ from (3.9) and (3.10) gives

$$\cos(\omega_0\tau) = \frac{(\theta a_2 - a_0 a_1)\omega_0^2}{(\theta a_2)^2 + a_1^2\omega_0^2}, \tag{3.12}$$

where ω_0 is given by the positive square root of (3.11).

So all the roots of (3.8) have negative real parts for $\tau = 0$, and $\widehat{\tau}$ is the smallest positive delay that satisfies (3.12). Hence for all $0 \leq \tau < \widehat{\tau}$, the corresponding linear system is stable.

Local Hopf bifurcation analysis

Consider a characteristic equation of the form

$$f(\lambda, K_1, K_2, ..., K_n) = 0,$$

where $\lambda = \sigma + j\omega$ is a complex variable and the K_i's are system parameters. To satisfy the Hopf condition (8), with respect to a parameter K_i, we also need to satisfy the *transversality condition*, i.e.

$$\text{Re}\left(\frac{d\lambda}{dK_i}\right)\Bigg|_{K_i=K_{i,c}} \neq 0,$$

where $K_{i,c}$ is the critical value of the parameter K_i beyond which the system is driven to instability. Note that at $K_i = K_{i,c}$ the eigenvalues lie on the imaginary axis, and so $\sigma = 0$ and $\lambda = j\omega_0$.

The characteristic equation we consider is (3.8), i.e

$$\lambda^2 + a_0\lambda + (a_1\lambda + \theta a_2)\, e^{-\lambda\tau} = 0,$$

where the critical values of the parameters are obtained from (3.12). We now verify that the transversality condition is satisfied by the delay τ and the damping parameter θ.

Feedback delay as the bifurcation parameter

Differentiating (3.8) with respect to τ and rearranging gives

$$\lambda' = \frac{\lambda e^{-\lambda\tau}\,(a_1\lambda + \theta a_2)}{2\lambda + a_0 + e^{-\lambda\tau}\,(a_1 - a_1\lambda\tau - \theta a_2\tau)},$$

where $\lambda' = \frac{d\lambda}{d\tau}$. From (3.8),

$$e^{-\lambda\tau} = -\frac{\lambda^2 + a_0\lambda}{a_1\lambda + \theta a_2}.$$

Substituting for $e^{-\lambda\tau}$ and putting $\lambda = j\omega_0$, we get

$$\lambda' = \frac{\omega_0^2\left(\theta a_0 a_2 - \omega_0^2 a_1 + j\omega_0\left(a_0 a_1 + \theta a_2\right)\right)}{\theta a_0 a_2 - \omega_0^2\left(a_1 + \theta a_2\tau + a_0 a_1\tau\right) + j\omega_0\left(2\theta a_2 + \theta a_0 a_2\tau - \omega_0^2 a_1\tau\right)}.$$

It can be readily shown that

$$\text{sign}\left\{\text{Re}\left(\lambda'\right)\right\} = \text{sign}\left\{\theta^2 a_0^2 a_2^2 + 2\theta^2 a_2^2\omega_0^2 + a_1^2\omega_0^4\right\},$$

which is always positive. As the transversality condition is satisfied, the associated system will undergo a Hopf bifurcation for large values of the feedback delay.

Damping factor as the bifurcation parameter

Differentiating (3.8) with respect to θ and rearranging gives

$$\lambda' = \frac{-a_2 e^{-\lambda\tau}}{2\lambda + a_0 + e^{-\lambda\tau}\left(a_1 - a_1\tau\lambda - \theta a_2\tau\right)},$$

where $\lambda' = \frac{d\lambda}{d\theta}$. Substituting for $e^{-\lambda\tau}$ and putting $\lambda = j\omega_0$, we get

$$\lambda' = \frac{a_2\left(-\omega_0^2 + j\omega_0 a_0\right)}{\left(\theta a_0 a_2 - \omega_0^2\left(a_1 + \theta a_2\tau + a_0 a_1\tau\right)\right) + j\omega_0\left(2\theta a_2 + \theta a_0 a_2\tau - \omega_0^2 a_1\tau\right)}.$$

We can show that

$$\text{sign}\{\text{Re}(\lambda')\} = \text{sign}\left\{a_2\omega_0^2\left(\omega_0^2(a_1 + \theta a_2\tau) + \theta a_0 a_2(a_0\tau + 1)\right)\right\},$$

which is always positive since $a_0, a_1, a_2 > 0$. Thus variations in the damping factor θ can also induce a Hopf bifurcation. An important parameter in the C-TCP/AVQ model is θ, and variations in this parameter can lead to limit cycles in the underlying non-linear system.

We have just shown that a class of linear equations, whose characteristic equation is represented by (3.8), can lose stability with large delays and with variations in the parameter θ. Further, both the delay and θ can induce a Hopf bifurcation.

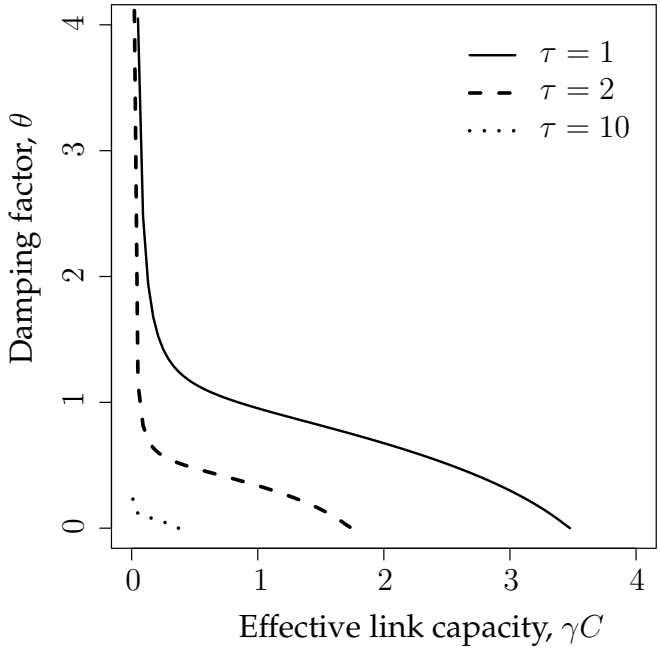

Figure 3.3: Local stability chart of the C-TCP/AVQ model. The area below the curves represents the stable region. Note the trade-offs among the system parameters to maintain stability. Variations in the AVQ damping factor θ can induce a Hopf bifurcation. Compound parameters: $\alpha = 0.125$, $\beta = 0.5$, $k = 0.75$.

Impact of delays on stability of C-TCP/AVQ

The local stability analysis of a TCP Reno/AVQ model was conducted in (10), which showed that large values of the delay can be destabilising. Following a similar style of analysis, one can identify a $\widehat{\tau}$ satisfying (3.12) such that for $\tau < \widehat{\tau}$, the C-TCP/AVQ system (3.5) is locally stable. Thus stability of the C-TCP/AVQ model will not be assured for large feedback delays.

Impact of the damping factor on stability of C-TCP/AVQ

A key parameter in the AVQ policy is the damping factor θ, which determines the rate of adaptation at the resource. Figure 3.3 shows a stability chart, highlighting the trade-offs between θ, the feedback delay and the effective link capacity to maintain local stability. In AVQ, adaptation at the links was introduced to target a high link utilisation at equilibrium. However, our analysis shows that variations in this parameter can induce a Hopf bifurcation in the C-TCP/AVQ model.

Discussion

Virtual queue policies are attractive as they can provide early indications of congestion to help end-systems adapt their rates. But this feature alone does not guarantee stability in the presence of time delayed feedback. We highlighted that small buffer thresholds help ensure stability, and would naturally reduce latency. We then exhibited that virtual queues, with small thresholds, have a stabilising effect but these thresholds have to be chosen in conjunction with Compound parameters. So stability can be ensured, but there is no explicit control over link utilisation.

The AVQ policy aims to achieve a desired link utilisation at equilibrium, and introduces a damping factor θ at the resource. However, at sufficiently high feedback delays the C-TCP/AVQ model is prone to losing local stability. In fact, an increase in θ can induce a loss of stability via a Hopf bifurcation.

From the analysis in the paper, our recommendation is that a non-adaptive virtual queue policy, with small virtual buffer sizing rules, is an attractive queue management scheme.

CHAPTER 4

Outlook

End-systems can detect congestion in the network via the loss of packets or by increased latency. Today, transport protocols like Compound TCP use both loss and delay as feedback to manage their flow and congestion control algorithms. Queueing delay, specially at network routers, is increasing which can be detrimental to services and applications that require low latency for good quality of service (11). Large buffers, without effective queue management, contribute fairly substantially to latency in the network (4). A plausible way to reduce latency from router buffers is to design appropriate Active Queue Management (AQM) schemes. We note that feedback to end-users is always time delayed, and so stability is a key performance metric.

Contributions

We studied some stability properties of a fluid model of the widely deployed Compound TCP with virtual queue policies. Our investigation of a non-adaptive Virtual Queue (VQ) revealed that small virtual buffer sizing rules would help stability, and also reduce network latency. We showed that Compound parameters can influence stability, and that unguided choice of parameters can easily violate the stability conditions. Analysis of the AVQ showed that large delays, high link capacities, and variations in the AVQ damping parameter can render the system in a locally unstable state. Additionally, we explicitly characterised the loss of local stability to occur via a Hopf bifurcation.

With a non-adaptive VQ we could have low latency and a stable system, but no explicit control over link utilisation. The AVQ is designed to target a desired and high link utilisation, but the AVQ damping factor can readily induce a Hopf bifurcation. Thus a simple non-adaptive virtual queue policy, with small router buffers, appears to be an appealing choice for queue management.

Avenues for further research

When a Hopf bifurcation condition is just violated, we can expect a limit cycle branching from the fixed point (6). It would be important to determine if the bifurcating limit cycle, with the AVQ, is asymptotically stable. One could follow the style of analysis presented in (8) (13) to address this question. Feedback to end-systems could also be in the form of Explicit Congestion Notification (ECN) (2). ECN allows routers to *mark* an IP packet when resources start to get congested. Thus end-systems do not need to rely only on packet loss, or latency, to infer the state of congestion in the network. It is natural to investigate the benefits of a virtual queue based scheme, with small router buffers, employing ECN marks.

APPENDIX A

Analytical characterisation: stability and periodicity of bifurcating solutions

In Section 3, we proved that variations in the damping parameter θ can induce a loss of stability in the C-TCP/AVQ system via a Hopf bifurcation. This leads to the emergence of limit cycles. The next question to address would be the nature of the Hopf and the stability of the ensuing limit cycles.

A Taylor expansion of the C-TCP/AVQ model (3.5) about the equilibrium point (3.6) yields

$$\begin{aligned}\frac{du(t)}{dt} &= -\frac{\alpha}{\tau}u(t) - \beta\tilde{C}^*u(t-\tau) + \beta w^* v(t-\tau) \\ &\quad - \frac{\beta}{\tau}u(t)u(t-\tau) - \frac{\beta\tilde{C}^*}{w^*}\left(u(t-\tau)\right)^2 \\ &\quad + \beta u(t)v(t-\tau) + \beta u(t-\tau)v(t-\tau) \\ \frac{dv(t)}{dt} &= -\frac{\theta}{\tau}u(t).\end{aligned}$$

We introduce an exogenous non-dimensional parameter $\kappa = \kappa_c + \mu$, where $\kappa_c = 1$, and the Hopf bifurcation occurs at $\mu = 0$. Substituting b_1, b_2, b_c, b_{12}, b_{22}, b_{1c} and b for $-\alpha/T$, $-\beta\tilde{C}^*$, βw^*, $-\frac{\beta}{\tau}$, $-\frac{\beta\tilde{C}^*}{w^*}$, β and $-\frac{\theta}{\tau}$ respectively, we have:

$$\begin{aligned}\frac{du(t)}{dt} &= \kappa b_1 u(t) + \kappa b_2 u(t-\tau) + \kappa b_c v(t-\tau) \\ &\quad + \kappa b_{12}u(t)u(t-\tau) + \kappa b_{22}\left(u(t-\tau)\right)^2 \\ &\quad + \kappa b_{1c}u(t)v(t-\tau) + \kappa b_{1c}u(t-\tau)v(t-\tau) \\ \frac{dv(t)}{dt} &= bu(t).\end{aligned} \tag{A.1}$$

We will now perform calculations that will enable us to address questions about the form of the bifurcating solutions of (A.1) as it transits from stability to instability via a Hopf bifurcation. We follow the style of analysis provided in (8).

Consider the following autonomous delay-differential system:

$$\frac{d}{dt}\boldsymbol{u}(t) = \mathcal{L}_\mu \boldsymbol{u}_t + \mathcal{F}(\boldsymbol{u}_t, \mu) \tag{A.2}$$

where $t > 0$, $\mu \in \mathbb{R}$, and for $T > 0$,

$$\boldsymbol{u}_t(\theta) = \boldsymbol{u}(t+\theta) \qquad \boldsymbol{u} : [-T, 0] \to \mathbb{R}^2, \qquad \theta \in [-T, 0].$$

$\mathcal{L}_\mu$ is a one-parameter family of continuous (bounded) linear operators. The operator $\mathcal{F}(\boldsymbol{u}_t, \mu)$ contains the non-linear terms. Further assume that $\mathcal{F}$ is analytic and that $\mathcal{F}$ and $\mathcal{L}_\mu$ depend analytically on the bifurcation parameter μ for small $|\mu|$. Note that (3.5) is of the form (A.2), where $\boldsymbol{u} = [u, c]^T$. The objective now is to cast (A.2) into the form:

$$\frac{d}{dt}\boldsymbol{u}_t = \mathcal{A}(\mu)\boldsymbol{u}_t + \mathcal{R}\boldsymbol{u}_t \tag{A.3}$$

which has $\boldsymbol{u}_t$ rather than both $\boldsymbol{u}$ and $\boldsymbol{u}_t$.

First, we transform the linear problem $d\boldsymbol{u}(t)/dt = \mathcal{L}_\mu \boldsymbol{u}_t$. From the Riesz representation theorem, there exists an $n \times n$ matrix function $\eta(\cdot, \mu) : [-T, 0] \to \mathbb{R}^{n^2}$, such that the components of η have bounded variation and for all $\boldsymbol{\phi} \in C[-T, 0]$,

$$\mathcal{L}_\mu \boldsymbol{\phi} = \int_{-T}^{0} d\eta(\theta, \mu)\boldsymbol{\phi}(\theta).$$

In particular,

$$\mathcal{L}_\mu \boldsymbol{\phi} = \int_{-T}^{0} d\eta(\theta, \mu)\boldsymbol{u}(t+\theta). \tag{A.4}$$

Observe that

$$d\eta(\theta, \mu) = \begin{bmatrix} (\kappa b_1 \delta(\theta) + \kappa b_2 \delta(\theta + \tau))d\theta & \kappa b_c \delta(\theta + \tau)d\theta \\ b\delta(\theta)d\theta & 0 \end{bmatrix}$$

satisfies (A.4). For $\boldsymbol{\phi} \in C[-T, 0]$, define

$$\mathcal{A}(\mu)\boldsymbol{\phi}(\theta) = \begin{cases} \frac{d\boldsymbol{\phi}(\theta)}{d\theta}, & \theta \in [-T, 0] \\ \int_{-T}^{0} d\eta(s, \mu)\boldsymbol{\phi}(s) \equiv \mathcal{L}_\mu \boldsymbol{\phi}, & \theta = 0 \end{cases} \tag{A.5}$$

and

$$\mathcal{R}\boldsymbol{\phi}(\theta) = \begin{cases} 0, & \theta \in [-T, 0] \\ \mathcal{F}(\boldsymbol{\phi}, \mu), & \theta = 0. \end{cases} \tag{A.6}$$

As $d\boldsymbol{u}_t/d\theta = d\boldsymbol{u}_t/dt$, (A.2) becomes (A.3) as desired.

The bifurcating periodic solutions $\boldsymbol{u}\big(t, \mu(\epsilon)\big)$ of (A.2) have amplitude $\mathcal{O}(\epsilon)$ and non-zero Floquet exponent $\mathcal{B}(\epsilon)$, where the expressions for μ and $\mathcal{B}$ are given by

$$\mu = \mu_2\epsilon^2 + \mu_4\epsilon^4 + \cdots$$
$$\mathcal{B} = \mathcal{B}_2\epsilon^2 + \mathcal{B}_4\epsilon^4 + \cdots .$$

The sign of μ_2 determines the direction of bifurcation. $\mu_2 > 0$ represents a supercritical bifurcation and $\mu_2 < 0$, a subcritical one. The sign of $\mathcal{B}_2$ determines the stability of the limit cycle. Asymptotic orbital stability is maintained if $\mathcal{B}_2 < 0$, and it is unstable otherwise. These coefficients will now be determined.

We only need to compute the expressions at $\mu = 0$, hence we set $\mu = 0$. Let $\boldsymbol{q}(\theta)$ be the eigenfunction for $\mathcal{A}(0)$ corresponding to $\lambda(0)$, namely

$$\mathcal{A}(0)\boldsymbol{q}(\theta) = i\omega_0\boldsymbol{q}(\theta)$$

To find ω_0 and $\boldsymbol{q}(\theta)$, let $\boldsymbol{q}(\theta) = \boldsymbol{q}_0 e^{i\omega_0\theta}$, where $\boldsymbol{q}_0 = [1, q_{02}]^T$. Substituting this in the above equation and using the expression for $\mathcal{A}$ as in (A.5), we get:

$$\begin{aligned} \omega_0 &= \sqrt{\frac{(b_2^2 - b_1^2) + \sqrt{(b_2^2 - b_1^2)^2 + 4b_c^2}}{2}} \\ \boldsymbol{q}_0 &= \begin{bmatrix} 1 \\ \frac{b}{i\omega} \end{bmatrix} \equiv \begin{bmatrix} q_{01} \\ q_{02} \end{bmatrix} \end{aligned} \tag{A.7}$$

Define the adjoint operator $\mathcal{A}^*(0)$ as

$$\mathcal{A}^*(0)\boldsymbol{\alpha}(s) = \begin{cases} \frac{d\boldsymbol{\alpha}(s)}{ds}, & s \in [0, T] \\ \int_{-T}^{0} d\eta^T(t, 0)\boldsymbol{\alpha}(-t), & s = 0. \end{cases}$$

Note that the domains of $\mathcal{A}$ and $\mathcal{A}^*$ are $C^1[-T,0]$ and $C^1[0,T]$ respectively. As

$$\mathcal{A}(0)\boldsymbol{q}(\theta) = \lambda(0)\boldsymbol{q}(\theta),$$

$\overline{\lambda}(0)$ is an eigenvalue for $\mathcal{A}^*$, and

$$\mathcal{A}^*(0)\boldsymbol{q}^* = -i\omega_0\boldsymbol{q}^*$$

for some non-zero vector $\boldsymbol{q}^*$. For $\boldsymbol{\phi} \in C[-T,0]$ and $\boldsymbol{\psi} \in C[0,T]$, define an inner product

$$\langle \boldsymbol{\psi}, \boldsymbol{\phi} \rangle = \overline{\boldsymbol{\psi}}^T(0)\boldsymbol{\phi}(0) - \int_{\theta=-T}^{0}\int_{\tau=0}^{\theta} \overline{\boldsymbol{\psi}}^T(\tau-\theta)d\eta(\theta)\boldsymbol{\phi}(\tau)d\tau. \tag{A.8}$$

Then, $\langle \boldsymbol{\psi}, \mathcal{A}\boldsymbol{\phi} \rangle = \mathcal{A}^*\langle \boldsymbol{\psi}, \boldsymbol{\phi} \rangle$ for $\boldsymbol{\phi} \in \mathrm{Dom}(\mathcal{A})$ and $\boldsymbol{\psi} \in \mathrm{Dom}(\mathcal{A})$.

Let $\boldsymbol{q}^*(s) = De^{i\omega_0 s}$ be an eigenvector of $\mathcal{A}^*$ corresponding to eigenvalue $-i\omega_0$. We will now find D such that the eigenvectors $\boldsymbol{q}$ and $\boldsymbol{q}^*$ satisfy conditions $\langle \boldsymbol{q}^*, \boldsymbol{q} \rangle = 1$ and $\langle \boldsymbol{q}^*, \overline{\boldsymbol{q}} \rangle = 0$. These two equations can be solved for variables D_1 and D_2, where $\boldsymbol{D} = [D_1, D_2]^T$.

Following the analysis similar to the one leading to (A.7), we find that

$$\boldsymbol{q^*}_0 = D_1 \begin{bmatrix} 1 & \frac{b_1 b_c + i\omega_0 b_c}{-bb_c + ib_2} \end{bmatrix}. \tag{A.9}$$

Using the expression (A.8) for the inner product and on solving for D_1, we get

$$D_1 = \frac{i\omega_0\left(bb_c + i\omega_0 b_2\right)}{\omega_0^2\left(b_1 b_2 + bb_c - b_2\right) - b_1 b_c b + 2i\omega_0 bb_c - e^{-i\omega_0\tau}\left(bb_c + i\omega_0 b_2\right)^2}. \tag{A.10}$$

For $\boldsymbol{u}_t$, a solution of (A.3) at $\mu = 0$, define

$$z(t) = \langle \boldsymbol{q}^*, \boldsymbol{u}_t \rangle$$
$$\boldsymbol{w}(t,0) = \boldsymbol{u}_t(\theta) - 2\mathcal{RE}(z(t)\boldsymbol{q}(\theta)).$$

Then, on the manifold, C_0, $\boldsymbol{w}(t,\theta) = \boldsymbol{w}(z(t), \overline{z}(t), \theta)$, where

$$\boldsymbol{w}(z,\overline{z},\theta) = \boldsymbol{w}_{20}(\theta)\frac{z^2}{2} + \boldsymbol{w}_{11}(\theta)z\overline{z} + \boldsymbol{w}_{02}(\theta)\frac{\overline{z}^2}{2} + \cdots. \tag{A.11}$$

In effect, z and $\overline{z}$ are local coordinates for C_0 in C in the directions of $\boldsymbol{q}^*$ and $\overline{\boldsymbol{q}}^*$, respectively. Note that $\boldsymbol{w}$ is real if $\boldsymbol{u}_t$ is real and we deal only with real

solutions. The existence of the centre manifold enables the reduction of (A.3) to an ordinary differential equation for a single complex variable on C_0. At $\mu = 0$,

$$\begin{aligned} z^{'}(t) &= \langle \boldsymbol{q}^*, \mathcal{A}\boldsymbol{u}_t + \mathcal{R}\boldsymbol{u}_t \rangle \\ &= i\omega_0 z(t) + \overline{\boldsymbol{q}}_*(0) \cdot \mathcal{F}\Big(\boldsymbol{w}(z,\overline{z},\theta) + 2\mathcal{R}\mathcal{E}\big(z\boldsymbol{q}(\theta)\big)\Big) \\ &= i\omega_0 z(t) + \overline{\boldsymbol{q}}_*(0) \cdot \mathcal{F}_{\prime}(z,\overline{z}), \end{aligned} \tag{A.12}$$

which can be abbreviated to

$$z^{'}(t) = i\omega_0 z(t) + g(z,\overline{z}). \tag{A.13}$$

The next objective is to expand g in powers of z and $\overline{z}$. However, we also have to determine the coefficients $\boldsymbol{w}_{ij}(\theta)$ in (A.11). Once the $\boldsymbol{w}_{ij}$ have been determined, the differential equation (A.12) for z would be explicit [as abbreviated in (A.12)] where expanding $g(z,\overline{z})$ in powers of z and $\overline{z}$, we have

$$\begin{aligned} g(z,\overline{z}) &= \overline{\boldsymbol{q}}^*(0) \cdot \mathcal{F}_0(z,\overline{z}) \\ &= g_{20}\frac{z^2}{2} + g_{11}z\overline{z} + g_{02}\frac{\overline{z}^2}{2} + g_{21}\frac{z^2\overline{z}}{2}\cdots . \end{aligned}$$

Following (8), we write

$$\boldsymbol{w}^{'} = u_t^{'} - z^{'}\boldsymbol{q} - \overline{z}^{'}\overline{\boldsymbol{q}}$$

and using (A.3) and (A.13), we obtain

$$\boldsymbol{w}^{'} = \begin{cases} \mathcal{A}\boldsymbol{w} - 2\mathcal{R}\mathcal{E}\left(\overline{\boldsymbol{q}}^*(0)\cdot\mathcal{F}_0\boldsymbol{q}(\theta)\right), & \theta \in [-T, 0] \\ \mathcal{A}\boldsymbol{w} - 2\mathcal{R}\mathcal{E}\left(\overline{\boldsymbol{q}}^*(0)\cdot\mathcal{F}_0 q(0)\right) + \mathcal{F}_0, & \theta = 0 \end{cases}$$

which is rewritten as

$$\mathbf{w}^{'} = \mathcal{A}\boldsymbol{w} + \boldsymbol{h}(z,\overline{z},\theta) \tag{A.14}$$

using (A.11), where

$$\boldsymbol{h}(z,\overline{z},\theta) = \boldsymbol{h}_{20}(\theta)\frac{z^2}{2} + \boldsymbol{h}_{11}(\theta)z\overline{z} + \boldsymbol{h}_{02}(\theta)\frac{\overline{z}^2}{2} + \cdots . \tag{A.15}$$

Now on C_0, near the origin,

$$\boldsymbol{w}^{'} = \boldsymbol{w}_z z^{'} + \boldsymbol{w}_{\overline{z}} \overline{z}^{'}.$$

Using (A.11) and (A.13) to replace $\boldsymbol{w}_z$, $z^{'}$ (and their conjugates by their power series expansion) and equating this with (A.14), we get

$$\begin{aligned} (2i\omega_0 - \mathcal{A})\boldsymbol{w}_{20}(\theta) &= \boldsymbol{h}_{20}(\theta) \\ -\mathcal{A}\boldsymbol{w}_{11}(\theta) &= \boldsymbol{h}_{11}(\theta) \\ -(2i\omega_0 + \mathcal{A})\boldsymbol{w}_{02}(\theta) &= \boldsymbol{h}_{02}(\theta). \end{aligned} \tag{A.16}$$

We start by observing

$$\begin{aligned} \boldsymbol{u}_t(\theta) &= \boldsymbol{w}(z, \overline{z}, \theta) + \boldsymbol{q}(\theta) z + \overline{\boldsymbol{q}}(\theta)\overline{z} \\ &= \boldsymbol{w}_{20}(\theta)\frac{z^2}{2} + \boldsymbol{w}_{11}(\theta) z\overline{z} + \boldsymbol{w}_{02}(\theta)\frac{\overline{z}^2}{2} \\ &\quad + \boldsymbol{q}_0 e^{i\omega_0\theta} z + \overline{\boldsymbol{q}}_0 e^{-i\omega_0\theta}\overline{z} + \cdots \end{aligned}$$

from which we obtain $\boldsymbol{u}_t(0)$ and $\boldsymbol{u}_t(-T)$. We have actually looked ahead and we will only be requiring the coefficients of z^2, $z\overline{z}$, $\overline{z}^2$, $z^2\overline{z}$, hence we keep only the relevant terms in the expansions that follow. We see that we have four non-linear terms:

$$\begin{aligned} u(0)\,u(-\tau) &= \begin{bmatrix} u(0)\,u(-\tau) & u(0)\,v(-\tau) \\ v(0)\,u(-\tau) & v(0)\,v(-\tau) \end{bmatrix}_{11} \\ &= e^{-i\omega_0\tau} z^2 + e^{i\omega_0\tau}\bar{z}^2 + \sin(\omega_0\tau)\, z\bar{z} \\ &\quad + \left(\frac{w_{201}(0)}{2} e^{i\omega_0\tau} + w_{111}(0) e^{-i\omega_0\tau} \right. \\ &\quad \left. + w_{111}(-\tau) + \frac{w_{201}(-\tau)}{2} \right) z^2\bar{z} \end{aligned}$$

$$
\begin{aligned}
u\left(-\tau\right)u\left(-\tau\right) &= \begin{bmatrix} u\left(-\tau\right)u\left(-\tau\right) & u\left(-\tau\right)v\left(-\tau\right) \\ v\left(-\tau\right)u\left(-\tau\right) & v\left(-\tau\right)v\left(-\tau\right) \end{bmatrix}_{11} \\
&= e^{-2i\omega_0\tau}z^2 + e^{2i\omega_0\tau}\bar{z}^2 + 2z\bar{z} + z^2\bar{z} \\
&\quad \times \left(w_{201}\left(-\tau\right)e^{i\omega_0\tau} + 2w_{111}\left(-\tau\right)e^{-i\omega_0\tau}\right) \\
u\left(0\right)v\left(-\tau\right) &= \begin{bmatrix} u\left(0\right)u\left(-\tau\right) & u\left(0\right)v\left(-\tau\right) \\ v\left(0\right)u\left(-\tau\right) & v\left(0\right)v\left(-\tau\right) \end{bmatrix}_{12} \\
&= q_{02}e^{-i\omega_0\tau}z^2 + \bar{q}_{02}e^{i\omega_0\tau}\bar{z}^2 \\
&\quad + \left(q_{02}e^{-i\omega_0\tau} + \bar{q}_{02}e^{i\omega_0\tau}\right)z\bar{z} \\
&\quad + \left(\frac{w_{201}(0)\bar{q}_{02}}{2}e^{i\omega_0\tau} + w_{111}(0)q_{02}e^{-i\omega_0\tau}\right. \\
&\quad \left. + w_{112}(-\tau) + \frac{w_{202}(-\tau)}{2}\right)z^2\bar{z} \\
u\left(-\tau\right)v\left(-\tau\right) &= \begin{bmatrix} u\left(-\tau\right)u\left(-\tau\right) & u\left(-\tau\right)v\left(-\tau\right) \\ v\left(-\tau\right)u\left(-\tau\right) & v\left(-\tau\right)v\left(-\tau\right) \end{bmatrix}_{12} \\
&= q_{02}e^{-2i\omega_0\tau}z^2 + \bar{q}_{02}e^{2i\omega_0\tau}\bar{z}^2 \\
&\quad + \left(q_{02} + \bar{q}_{02}\right)z\bar{z} + \left(\frac{w_{201}(-\tau)\bar{q}_{02}}{2}e^{i\omega_0\tau}\right. \\
&\quad + w_{111}(-\tau)q_{02}e^{-i\omega_0\tau} + w_{112}(-\tau)e^{-i\omega_0\tau} \\
&\quad \left. + \frac{w_{202}(-\tau)e^{i\omega_0\tau}}{2}\right)z^2\bar{z},
\end{aligned}
$$

where $[w_{ij1}, w_{ij2}]^T = \boldsymbol{w}_{ij}$. Recall that,

$$
g(z,\overline{z}) = \overline{\boldsymbol{q}}^*(0)\cdot\mathcal{F}_0(z,\overline{z}) \equiv \overline{D}_1\mathcal{F}_{01}(z,\overline{z}),
$$

where $[\mathcal{F}_{01}, \mathcal{F}_{02}]^T = \mathcal{F}_0$, and

$$
g(z,\overline{z}) = g_{20}\frac{z^2}{2} + g_{11}z\overline{z} + g_{02}\frac{\overline{z}^2}{2} + g_{21}\frac{z^2\overline{z}}{2}\cdots.
$$

Comparing the two equations above, we get:

$$\begin{aligned} g_{02} =& 2D_1\kappa\big(b_{12}e^{i\omega_0\tau} + b_{22}e^{2i\omega_0\tau} \\ &+ b_{1c}\bar{q}_{02}\left(e^{i\omega_0\tau} + e^{2i\omega_0\tau}\right)\big) \end{aligned} \tag{A.17}$$

$$\begin{aligned} g_{11} =& D_1\kappa\big(2b_{12}\cos\left(\omega_0\tau\right) + 2b_{22} + b_{1c}\big(\bar{q}_{02}\left(1 + e^{i\omega_0\tau}\right) \\ &+ q_{02}\left(1 + e^{-i\omega_0\tau}\right)\big)\big) \end{aligned} \tag{A.18}$$

$$\begin{aligned} g_{20} =& 2D_1\kappa\big(b_{12}e^{-i\omega_0\tau} + b_{22}e^{-2i\omega_0\tau} \\ &+ b_{1c}q_{02}\left(e^{-i\omega_0\tau} + e^{-2i\omega_0\tau}\right)\big) \end{aligned} \tag{A.19}$$

$$\begin{aligned} g_{21} =& D_1\kappa\Bigg(b_{12}\Big(w_{201}\left(0\right)e^{i\omega_0\tau} + 2w_{111}\left(0\right)e^{-i\omega_0\tau} \\ &+ 2w_{111}\left(-\tau\right) + w_{201}\left(-\tau\right)\Big) \\ &+ b_{22}\left(2w_{201}\left(-\tau\right)e^{i\omega_0\tau} + 4w_{111}\left(-\tau\right)e^{-i\omega_0\tau}\right) \\ &+ b_{1c}\Big(w_{201}\left(-\tau\right)\left(1 + e^{i\omega_0\tau} + \bar{q}_{02}e^{i\omega_0\tau}\right) \\ &+ w_{201}\left(0\right)e^{i\omega_0\tau}\left(1 + \bar{q}_{02}\right) \\ &+ 2w_{111}\left(0\right)e^{-i\omega_0\tau}\left(1 + q_{02}\right) \\ &+ w_{202}\left(-\tau\right)\left(1 + e^{i\omega_0\tau}\right) \\ &+ 2w_{111}\left(-\tau\right)\left(1 + 2e^{-i\omega_0\tau} + q_{02}e^{-i\omega_0\tau}\right) \\ &+ 2w_{112}\left(-\tau\right)\left(1 + e^{-i\omega_0\tau}\right)\Big)\Bigg) \end{aligned}$$

For the expression of g_{21}, we still need to evaluate $\boldsymbol{w}_{11}(0)$, $\boldsymbol{w}_{11}(-T)$, $\boldsymbol{w}_{20}(0)$ and $\boldsymbol{w}_{20}(-T)$. Now for $\theta \in [-T, 0)$,

$$\begin{aligned} \boldsymbol{h}(z,\overline{z},\theta) &= -2\mathcal{RE}\left(\overline{\boldsymbol{q}}^*(0)\cdot\mathcal{F}_0\boldsymbol{q}(\theta)\right) \\ &= -2\mathcal{RE}\left(g(z,\overline{z})\boldsymbol{q}(\theta)\right) \\ &= -g\left(z,\overline{z}\right)\boldsymbol{q}(\theta) - \overline{g}(z,\overline{z})\overline{\boldsymbol{q}}(\theta) \\ &= \left(g_{20}\frac{z^2}{2} + g_{11}z\overline{z} + g_{02}\frac{\overline{z}^2}{2}\right)\boldsymbol{q}(\theta) \\ &- \left(\overline{g}_{20}\frac{z^2}{2} + \overline{g}_{11}z\overline{z} + \overline{g}_{02}\frac{\overline{z}^2}{2}\right)\overline{\boldsymbol{q}}(\theta), \end{aligned}$$

which, compared with (A.15), yields

$$\boldsymbol{h}_{20}(\theta) = -g_{20}\boldsymbol{q}(\theta) - g_{02}\overline{\boldsymbol{q}}(\theta)$$
$$\boldsymbol{h}_{11}(\theta) = -g_{11}\boldsymbol{q}(\theta) - g_{11}\overline{\boldsymbol{q}}(\theta).$$

From (A.5) and (A.16), we get

$$\boldsymbol{w}_{20}^{'}(\theta) = 2i\omega_0\boldsymbol{w}_{20}(\theta) + g_{20}\boldsymbol{q}(\theta) + \overline{g}_{02}\overline{\boldsymbol{q}}(\theta) \tag{A.20}$$
$$\boldsymbol{w}_{11}^{'}(\theta) = g_{11}\boldsymbol{q}(\theta) + \overline{g}_{11}\overline{\boldsymbol{q}}(\theta). \tag{A.21}$$

Solving the differential equations (A.20) and (A.21), we obtain:

$$\boldsymbol{w}_{20}(\theta) = -\frac{g_{20}}{i\omega_0}\boldsymbol{q}_0 e^{i\omega_0\theta} - \frac{\overline{g}_{02}}{3i\omega_0}\overline{\boldsymbol{q}}_0 e^{-i\omega_0\theta} + \boldsymbol{e}e^{2i\omega_0\theta} \tag{A.22}$$
$$\boldsymbol{w}_{11}(\theta) = \frac{g_{11}}{i\omega_0}\boldsymbol{q}_0 e^{i\omega_0\theta} - \frac{\overline{g}_{11}}{i\omega_0}\overline{\boldsymbol{q}}_0 e^{-i\omega_0\theta} + \boldsymbol{f} \tag{A.23}$$

for some $\boldsymbol{e} = [e_1, e_2]^T$ and $\boldsymbol{f} = [f_1, f_2]^T$, which we will determine now. For $\boldsymbol{h}(z, \overline{z}, 0) = -2\mathcal{RE}\left(\overline{\boldsymbol{q}}^*(0) \cdot \mathcal{F}_0 q(0)\right) + \mathcal{F}_0$,

$$\boldsymbol{h}_{20}(0) = -g_{20}q(0) - g_{02}\overline{\boldsymbol{q}}(0) + \begin{bmatrix} g_{20}/D_1 \\ 0 \end{bmatrix}$$
$$\boldsymbol{h}_{11}(0) = -g_{11}q(0) - g_{11}\overline{\boldsymbol{q}}(0) + \begin{bmatrix} g_{11}/D_1 \\ 0 \end{bmatrix}.$$

Again, from (A.5) and (A.16), we obtain

$$g_{20}\boldsymbol{q}(0) + g_{02}\overline{\boldsymbol{q}}(0) = \begin{bmatrix} g_{20}/D_1 \\ 0 \end{bmatrix} + \begin{bmatrix} \kappa b_1 w_{201}(0) + \kappa b_2 w_{201}(-\tau) + \kappa b_c w_{202}(-\tau) - 2i\omega_0 w_{201}(0) \\ b w_{201}(0) - 2i\omega_0 w_{202}(0) \end{bmatrix} \tag{A.24}$$

$$g_{11}\boldsymbol{q}(0) + g_{11}\overline{\boldsymbol{q}}(0) = \begin{bmatrix} g_{11}/D_1 \\ 0 \end{bmatrix} + \begin{bmatrix} \kappa b_1 w_{111}(0) + \kappa b_2 w_{111}(-\tau) + \kappa b_c w_{112}(-\tau) \\ b w_{111}(0) \end{bmatrix}. \tag{A.25}$$

Substituting the expression for $w_{ijk}(x), x \in [-T, 0]$ from (A.22) and (A.23) into (A.24) and (A.25), and finally solving for e_1, e_2, f_1 and f_2, we obtain:

$$\boldsymbol{e} \equiv \begin{bmatrix} e_1 \\ e_2 \end{bmatrix} = \begin{bmatrix} \frac{n_1 m_2 - n_2 m_1}{l_1 m_2 - l_2 m_1} \\ \frac{n_1 l_2 - n_2 l_1}{l_2 m_1 - l_1 m_2} \end{bmatrix} \tag{A.26}$$

and

$$\boldsymbol{f} \equiv \begin{bmatrix} f_1 \\ f_2 \end{bmatrix} = \begin{bmatrix} \left(\bar{g}_{11} - g_{11}\right)/i\omega_0 \\ \left(2 - \frac{1}{D_1}\right)\frac{g_{11}}{\kappa} + \frac{b}{\omega_0^2}\left(g_{11}e^{-i\omega_0\tau} + \bar{g}_{11}e^{i\omega_0\tau}\right) - b_2 w_{111}\left(-\tau\right) \end{bmatrix} \tag{A.27}$$

where

$$\begin{aligned} l_1 &= b,\ m_1 = -2i\omega_0,\ n_1 = \frac{g_{20} - g_{02}}{g_{20} - \bar{g}_{02}}, \\ l_2 &= \kappa e^{-2i\omega_0\tau}\left(b_1 + b_2\right) - 2i\omega_0,\ m_2 = \kappa b_c e^{-2i\omega_0\tau}, \\ n_2 &= g_{20}\left(1 - \frac{1}{D_1}\right) + g_{02} + \frac{\kappa b_1}{i\omega_0}\left(g_{20} + \frac{\bar{g}_{02}}{3} - 2i\omega_0\right) \\ &\quad + \frac{\kappa b_2}{i\omega_0}\left(g_{20}e^{-i\omega_0\tau} + \frac{\bar{g}_{02}}{3}e^{i\omega_0\tau}\right) - \frac{\kappa b_c b}{\omega_0^2}\left(g_{20}e^{-i\omega_0\tau} - \frac{\bar{g}_{02}}{3}e^{i\omega_0\tau}\right) \end{aligned}.$$

Using the values of $\boldsymbol{e}$ and $\boldsymbol{f}$ in (A.22) and (A.23), followed by substituting $\theta = 0$ and $-T$, we can obtain the values for $\boldsymbol{w}_{11}(0)$, $\boldsymbol{w}_{11}(-T)$, $\boldsymbol{w}_{20}(0)$ and $\boldsymbol{w}_{20}(-T)$. Using these, g_{21} can be evaluated. Hence, we finally have the expressions for g_{20}, g_{11}, g_{02} and g_{21}.

We now compute the values of $\alpha'(0) = \mathcal{RE}\left(\frac{d\lambda}{d\kappa}\right)$ and $\omega'(0) = \mathcal{IM}\left(\frac{d\lambda}{d\kappa}\right)$ at $\kappa = \kappa_c$, where $\mathcal{IM}(x)$ denotes the imaginary part of x. We start with our characteristic equation (3.7)

$$\lambda^2 + \kappa a_0\lambda + \kappa a_1\lambda e^{-\lambda\tau} + \kappa\theta a_2 e^{-\lambda\tau} = 0.$$

Substituting $\lambda = j\omega_0$, differentiating and rearranging using (8), we obtain

$$\frac{d\lambda}{d\kappa} = \frac{-\omega_0^2\left(a_2 + j\omega_0 a_1\right)}{\left(a_0 + 2i\omega_0\right)\left(a_2 + j\omega_0 a_1\right) + j\omega_0\left(a_0 + j\omega_0\right)\left(\tau a_2 - a_1 + j\omega_0 a_1 \tau\right)}.$$

We find that

$$\frac{d\lambda}{d\kappa} = \alpha^{'}(0) + j\omega^{'}(0).$$

This yields

$$\text{sign}\left(\frac{d\lambda}{d\kappa}\right) = \text{sign}\left(-\omega_0^2\left(a_0 a_2^2 - \omega_0^2\left(a_2\left(\tau a_2 - a_1\right)\right) - \omega_0^4\left(a_1^2\tau\right)\right)\right) \neq 0,$$

which proves the transversality condition with respect to κ. All the quantities required for the computations associated for the stability analysis of the Hopf bifurcation are completed. We can now comment on the nature of our Hopf bifurcation using the values of μ_2 and $\mathcal{B}_2$ (8)

$$\begin{aligned} \mu_2 &= \frac{-\mathcal{RE}\big(c_1(0)\big)}{\alpha^{'}(0)} \\ \mathcal{B}_2 &= 2\mathcal{RE}\big(c_1(0)\big), \end{aligned} \tag{A.28}$$

where, as in (8),

$$c_1(0) = \frac{i}{2\omega_0}\left(g_{20}g_{11} - 2|g_{11}|^2 - \frac{1}{3}|g_{02}|^2\right) + \frac{g_{21}}{2}. \tag{A.29}$$

Under the condition $\alpha^{'}(0) > 0$, if $\mathcal{RE}\big(c_1(0)\big) < 0$, then $\mu_2 > 0$ denotes a super-critical Hopf bifurcation and $\mathcal{B}_2 < 0$, a stable limit cycle, and vice versa. Also, the expression for the Floquet exponent $\mathcal{B}(\epsilon)$ is given by

$$\begin{aligned} \mathcal{B}(\epsilon) &= \mathcal{B}_2\epsilon^2 + \mathcal{O}\left(\epsilon^4\right), \\ \epsilon &= \sqrt{\frac{\mu}{\mu_2}}. \end{aligned} \tag{A.30}$$

For the C-TCP/AVQ system, consider the following values of the parameters at the Hopf condition:

$$\alpha = 0.125, \beta = 0.5, k = 1, \tau = 1, \gamma C = 2.7, \theta_c = 0.449.$$

The bifurcation parameter μ is chosen as $0.1\theta_c$. This yields

$$\mu_2 = -1.9, \beta_2 = 2.34. \tag{A.31}$$

Thus, the system undergoes a subcritical Hopf, and the ensuing limit cycles are unstable.

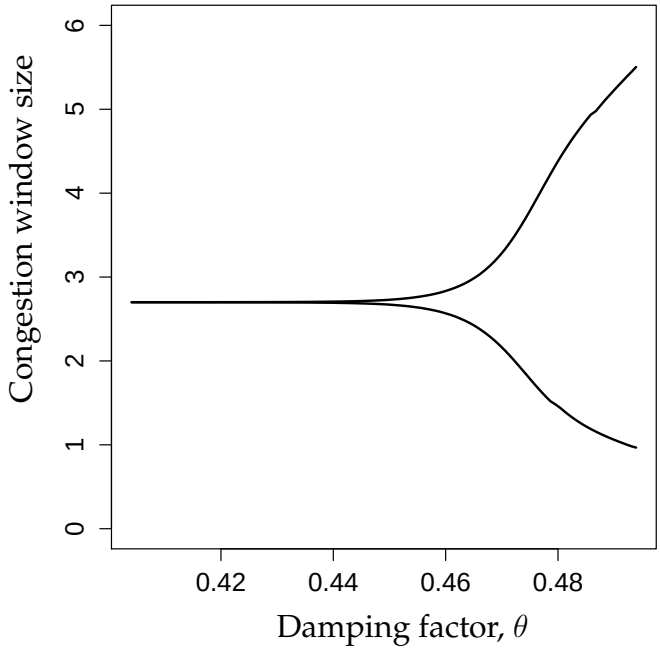

Figure A.1: Bifurcation diagram generated with variation in damping factor θ. The Hopf is found to be subcritical, and the limit cycles unstable (A.31).

REFERENCES

[1] S. Athuraliya, S.H. Low, V.H. Li, and Q. Yin, "REM: Active Queue Management", *IEEE Network*, vol. 15, pp. 48–53, 2001.

[2] S. Floyd, "TCP and explicit congestion notification", *ACM SIGCOMM Computer Communication Review*, vol. 24, pp. 8–23, 1994.

[3] S. Floyd and V. Jacobson, "Random Early Detection gateways for congestion avoidance", *IEEE/ACM Transactions on Networking*, vol. 1, pp. 397–413, 1993.

[4] J. Gettys and K. Nichols, "Bufferbloat: dark buffers in the Internet", *Communications of the ACM*, vol. 55, pp. 57–65, 2012.

[5] R.J. Gibbens and F.P. Kelly, "Resource pricing and the evolution of congestion control", *Automatica*, vol. 35, pp. 1969-1985, 1999.

[6] J. Guckenheimer and P. Holmes, *Nonlinear Oscillations, Dynamical Systems, and Bifurcations of Vector Fields*. New York: Springer-Verlag, 1983.

[7] J.M. Harrison, *Brownian Motion and Stochastic Flow Systems*. New York: Wiley, 1985.

[8] B.D. Hassard, N.D. Kazarinoff and Y. Wan, *Theory and Applications of Hopf Bifurcation*. Cambridge, U.K.: Cambridge University Press, 1981.

[9] F.P. Kelly, "Models for a self–managed Internet", *Philosophical Transactions of the Royal Society A*, vol. 358, pp. 2335–2348, 2000.

[10] S. Kunniyur and R. Srikant, "Analysis and design of an Adaptive Virtual Queue (AVQ) algorithm for Active Queue Management", *ACM SIGCOMM Computer Communication Review*, vol. 31, pp. 123–134, 2001.

[11] K. Nichols and V. Jacobson, "Controlling queue delay", *Communications of the ACM*, vol. 55, pp. 42–50, 2012.

[12] G. Patil, S. McClean and G. Raina, "Drop-Tail and RED queue management with small buffers: stability and Hopf bifurcation", *Journal on Communication Technology: Special Issue on Next Generation Wireless Networks and Applications*, vol. 2, pp. 339–344, 2011.

[13] G. Raina, "Local bifurcation analysis of some dual congestion control algorithms", *IEEE Transactions on Automatic Control*, vol. 50, pp. 1135–1146, 2005.

[14] G. Raina, D. Towsley and D. Wischik, "Part II: Control theory for buffer sizing", *ACM SIGCOMM Computer Communication Review*, vol. 35, pp. 79–82, 2005.

[15] G. Raina and D. Wischik, "Buffer sizes for large multiplexers: TCP queueing theory and instability analysis", in *Proceedings of Next Generation Internet Networks*, 2005.

[16] P. Raja and G. Raina, "Delay and loss-based transport protocols: buffer-sizing and stability", in *Proceedings of International Conference on Communication Systems and Networks*, 2012.

[17] K. Tan, J. Song, Q. Zhang and M. Sridharan, "A Compound TCP approach for high-speed and long distance networks", in *Proceedings of IEEE INFOCOM*, 2006.